PERGAMON

International Journal of Heat and Mass Transfer 43 (2000) 2553–2564

International Journal of HEAT and MASS TRANSFER

www.elsevier.com/locate/ijhmt

Condensation of R134a flowing inside helicoidal pipe

H.J. Kang, C.X. Lin, M.A. Ebadian*

Hemispheric Center for Environmental Technology, Florida International University, Miami, FL 33174, USA

Received 25 November 1998; received in revised form 17 September 1999

Abstract

Condensing heat transfer and pressure drop characteristics of an ozone-friendly refrigerant HFC-134a (hydrofluorocarbon 134a) flowing inside a 12.7 mm helicoidal tube were investigated experimentally to obtain heat transfer data and correlations. For long helicoidal pipe, heat transfer measurements were performed for the refrigerant flow mass fluxes from 100 to 400 kg/m^2/s, in the cooling water flow Reynolds number range of $1500 < Re_w < 9000$ at fixed system temperature (33°C) and cooling tube wall temperature (12°C and 22°C). With the increase of mass flux, the overall condensing heat transfer coefficients of R134a increased, and slowly the pressure drops also increased. However, with the increase of mass flux (or the cooling water flow Reynolds number), the refrigerant side heat transfer coefficients decreased. The effects of cooling wall temperature on heat transfer coefficients and system pressure drops were considered. Predictive correlations valid over the above water flow Reynolds number ranges and refrigerant flow mass flux were proposed. Helicoidal pipe heat transfer characteristics were compared with data for horizontal straight pipe from literature reports.

1. Introduction

Among the alternatives for CFCs (chlorofluorocarbons), the HFC-134a (hydrofluorocarbon 134a) is the most practical and is ready for commercial use. Therefore, the reliable phase change heat transfer data for alternative refrigerants such as R134a are significant for the design of new systems and equipment that use the alternative refrigerants as the working fluid. The helicoidal pipe's high heat transfer efficiency and compact volume make it important in many engineering areas such as the petrochemical, biomedical, pharmaceutical, power generation, and aerospace industries as well as refrigeration and air conditioning. In most applications, gas–liquid two-phase flow occurs inside the pipe.

Currently, one of the most common working fluids for refrigeration and air conditioning systems is Freon-12. However, environmental concerns with stratospheric ozone depletion and greenhouse warming are forcing a major shift from Freon-12 to R134a in air conditioning and refrigeration systems. Since the conventional system operated with R134a is about 20–30% less efficient, one way to improve the efficiency of the condenser is to redesign the condenser coil. Therefore, the study of condensation heat transfer in helicoidal pipe is essential for design purposes.

The heat transfer characteristic of R134a condensation in helicoidal pipes has rarely been investigated. Investigations concerning boiling and condensation heat transfer of refrigerants such as R134a, R407c, R12, R22, R114, and their mixture in straight pipe or a double-pipe passage can be

* Corresponding author. Tel.: +1-305-348-3585; fax: +1-305-348-4176.

E-mail address: ebadian@eng.fiu.edu (M.A. Ebadian).

0017-9310/00/$ - see front matter
PII: S0017-9310(99)00296-3

Nomenclature

A	heat transfer area (m^2)
B	pitch (m)
Cp	specific heat (J/kg °C)
D	coil diameter (m)
D	tube diameter (m)
De	Dean number, defined in Eq. (9)
F	flow rate (m^3/s)
f	friction factor
H	heat transfer coefficient (W/m^2 °C)
h	enthalpy (kJ/kg)
L	total length of the helicoidal pipe (m)
m	mass flux (kg/m^2)
Nu	Nusselt number
P	pressure (Pa)
Pr	Prandtl number ($Cp\ \mu/k$)
Q	heat transfer rate (W/s)
q	heat flux (W/m^2)
Re	Reynolds number, defined in Eq. (10)
Re^*	modified Reynolds number, defined in Eq. (25)
R_t	heat transfer resistance of the tube wall (m^2 °C/W)
T	temperature (°C)
u	velocity (m/s)
x	vapor quality

Greek symbols

ρ	density (kg/m^3)
λ	heat conductivity (W/m °C)
μ	viscosity (kg/m s)
ΔT_m	logarithm mean temperature difference (°C)

Subscripts

D	pressure difference
f	Freon
in	inlet or inner
l	liquid
o	overall
out	outlet or outer
s	saturation
single	single-phase flow region
turn	phase change point
two	two-phase flow region
v	Freon vapor
w	water
wall	tube wall
1	external tube
2	internal tube

found in the open literature. Bokhanovskiy [1] carried out condensation inside a double-tube coiled heat exchanger with R12–R22 mixture. Findings indicated that in the region of low heat flux density, the average heat transfer coefficients of the R12–R22 mixture are lower than those of the pure refrigerants. Stocker and Koronta [2] experimentally investigated the heat transfer and flow characteristics of the condensation of R12–R114 mixtures inside a horizontal glass tube. No remarkable effect of composition on the flow pattern is observed in their photographs. Tandon et al. [3,4] proposed a flow regime map for the condensation of R12–R22 in a horizontal glass tube. In their map, the flow pattern is not affected by composition. They also proposed a correlation of the local heat transfer coefficient. Mochizuki et al. [5] presented a correlation of the average heat transfer coefficient of the condensation of R11–R113 mixtures.

Heat transfer experiments for straight pipe have been conducted by Eckels and Pate [6], Torikoshi et al. [7,8], Ebisu and Torikoshi [9], Uddin et al. [10], Liu [11,12], and more recently by Huerta et al. [13]. Yet the condensation heat transfer characteristics of R134a in helicoidal pipe have not been determined. The effect of the liquid flow rate on the relative heat transfer coefficient has not been carefully investigated. More information on wall temperature and the local heat transfer coefficient is needed to analyze the characteristics of heat transfer inside helicoidal pipes. The lengths of the tubes tested in the previous studies are relatively short and of limited use; in design, only Liu's [12] work for straight tube considered this point.

In this investigation, the condensation heat transfer of R134a in helicoidal pipe has been conducted in a newly designed condensation and boiling two-phase flow experimental setup. This study obtains the heat transfer and pressure drop from a relatively long test section measuring 5.6 m in length. The experimental results are reported in the following sections.

2. Experimental system

Experiments in condensation heat transfer of R134a were performed in the experimental system built at Florida International University's Hemispheric Center for Environmental Technology (FIU-HCET). A schematic of the experimental system is shown in Fig. 1. The system consisted of two loops: a refrigerant flow loop and a water cooling loop. The refrigerant was pumped from the storage tank to the boiler, where temperature-controlled electric heaters were used to heat the refrigerant from liquid to vapor. A bypass was installed around the pump to adjust the flow through the pipe to the regenerator in which the refrigerant was heated to a temperature slightly higher than the saturation temperature. The vapor then flowed to a vapor mass meter, where the mass flow rate of the vapor was measured. After the mass flow rate measurement, the vapor entered the helicoidal pipe, where cooling was applied and condensation heat transfer occurred. In the regenerator, the heating to vapor flow was controlled to maintain the saturation temperature of refrigerant at the entrance of the helicoidal pipe. During the experiment, the vapor may be fully liquefied, or some vapor may remain at the exit of the helicoidal pipe, depending on the cooling condition applied. An additional condenser was used to cool down the refrigerant from the exit of the helicoidal pipe. After the refrigerant was fully cooled down to liquid state, it returned to the storage tank to complete the loop. The coolant was introduced from the chilled water line through the pump to the shell side of the helicoidal pipe. After flowing through the helicoidal pipe, it then returned to the chilled water resource. The water flow was adjusted using a bypass, and the flow rate was measured with a flow meter.

The pressure and the temperature were measured at different locations for the refrigerant flow and water flow. All the readings were collected by the data acquisition systems and stored for data reduction. The locations of the temperature and pressure measurement are also shown in Fig. 1. The whole experimental system was insulated thermally from its surroundings by a 50-mm thick glass fiber blanket.

In addition, in order to observe the flow pattern, two sight glass windows were installed at the exit of the test helicoidal pipe and additional condenser.

The test section of the helicoidal pipe is shown in Fig. 2. Both the inner and outer tubes were made of copper. The inner diameter of the inner tube measured 12.7 mm, while the inner diameter of the outer is 21.2 mm. The coil diameter is 177.8 mm. The space between the inner and outer tubes measured 8.5 mm. The pitch of the helicoidal pipe is 34.9 mm. The number of turns in the helicoidal pipe totaled 10. The refrigerant flows through the inner tube, and the cooling water flows in the passage (shell) formed by the inner and outer tubes. The inlet and outlet temperatures of both the refrigerant and water were measured.

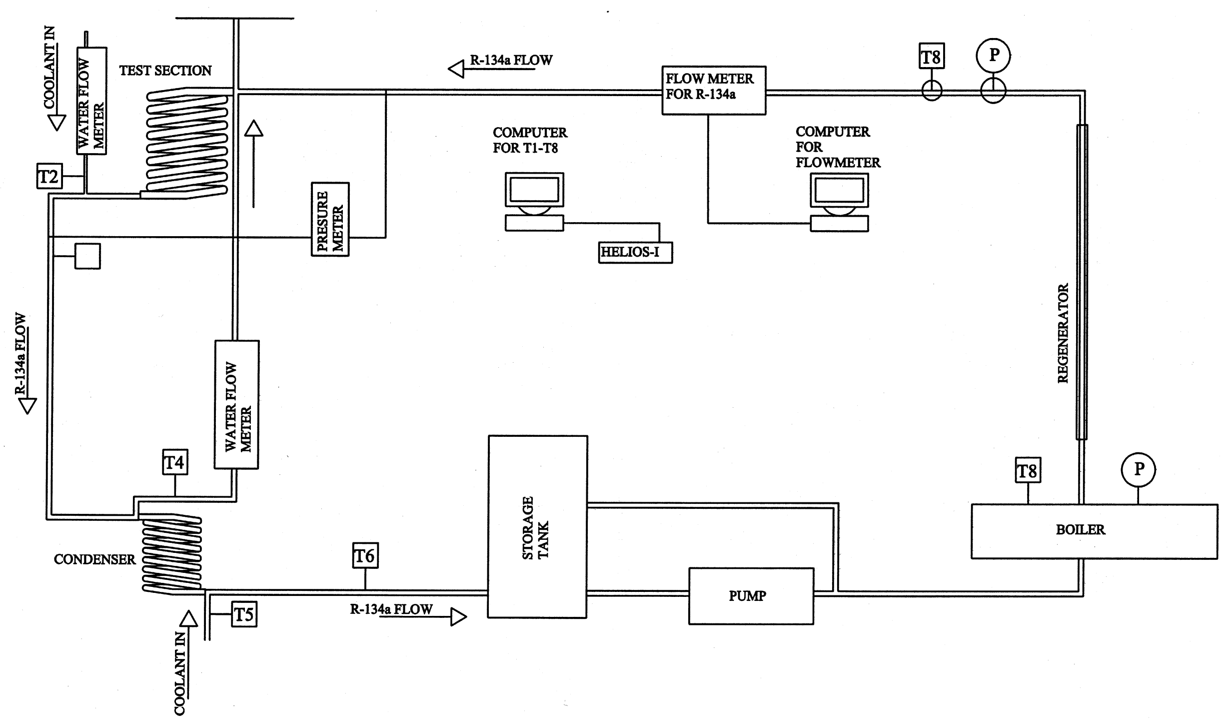

Fig. 1. Schematic of the test system.

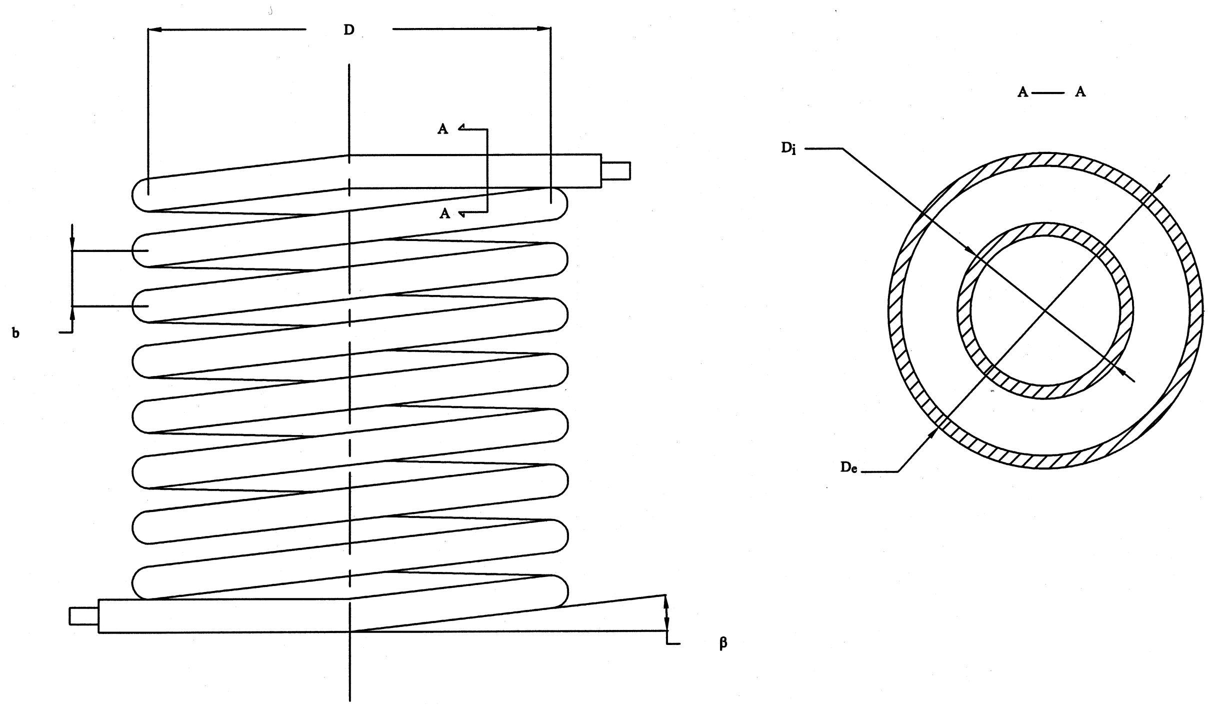

Fig. 2. Test section.

After the experimental system was thoroughly inspected for leakage, the refrigerant R134a was charged into the system. E-type and T-type thermocouples used in temperature measurement were calibrated before and after installation. Before installation, all thermocouples were calibrated against a precision thermometer with an accuracy of $\pm 0.1°C$. After installing the thermocouples on the insulated test sections, the thermocouples were calibrated again in situ at three fixed temperatures between 20°C and 60°C. The flow meters and the pressure gauges were also calibrated. The calibration factors for the R134a flow meter and for water flow meters were calculated as well.

The flow rates of the refrigerant and water were adjusted in each case. During the test, the heat balance between the heat released by the refrigerant and the heat absorbed by the water flow was calculated to verify that the system had reached steady condition. A heat balance deviation of 10% was considered acceptable. Once the steady state condition had been established, readings for the temperature, flow rate, and pressure were taken for 5 min. The average values of these data were used in the data reduction to obtain the heat transfer coefficient.

The thermal properties of the R134a were taken from the *Handbook of Fundamentals* [14]. The correlation has been obtained for each property as a function of temperature. Therefore, the data reduction can be fully computerized.

3. Data reduction method

According to the energy conservation principle, the amount of heat transfer from the refrigerant to the coolant can be determined from the enthalpy increase of coolant. Therefore, the heat transferred from the R134a to the water flows can be calculated from the following equation:

$$Q = F_{\mathrm{w}} \rho_{\mathrm{w}} Cp_{\mathrm{w}} \left(T_{\mathrm{w, out}} - T_{\mathrm{w, in}} \right) \tag{1}$$

Based on Newton's cooling law, the overall heat transfer coefficient can be determined by

$$Q = H_{\mathrm{o}} A \Delta T_{\mathrm{m}} = F_{\mathrm{w}} \rho_{\mathrm{w}} Cp_{\mathrm{w}} \left(T_{\mathrm{w, out}} - T_{\mathrm{w, in}} \right) \tag{2}$$

Thus,

$$H_{\mathrm{o}} = \frac{F_{\mathrm{w}} \rho_{\mathrm{w}} Cp_{\mathrm{w}} \left(T_{\mathrm{w, out}} - T_{\mathrm{w, in}} \right)}{A \Delta T_{\mathrm{m}}} \tag{3}$$

where ΔT_{m} is the logarithm mean temperature defined as

$$\Delta T_{\rm m}=\frac{\left(T_{\rm f,\,out}-T_{\rm w,\,in}\right)-\left(T_{\rm f,\,in}-T_{\rm w,\,out}\right)}{\ln\left[\left(T_{\rm f,\,out}-T_{\rm w,\,in}\right)/\left(T_{\rm f,\,in}-T_{\rm w,\,out}\right)\right]} \tag{4}$$

Actually, since the two-phase and single-phase flow coexist in the helicoidal pipe during the condensation process, $\Delta T_{\rm m}$ consists of two parts. One is for the two-phase flow region, and the other is for the single-phase flow region. The logarithm mean temperature difference $\Delta T_{\rm m,\,two}$ for the two-phase flow region is defined as

$$\Delta T_{\rm m,\,two}=\frac{\left(T_{\rm f,\,s}-T_{\rm w,\,in}\right)-\left(T_{\rm f,\,s}-T_{\rm w,\,turn}\right)}{\ln\left[\left(T_{\rm f,\,s}-T_{\rm w,\,in}\right)/\left(T_{\rm f,\,s}-T_{\rm w,\,turn}\right)\right]} \tag{5}$$

where $T_{\rm w,\,turn}$ is the temperature corresponding to the point at which two-phase flow turns to single-phase flow. The flow pattern change point can be identified with the energy balance method.

For the single-phase flow region, the logarithm mean temperature difference $\Delta T_{\rm m,\,single}$ is defined as

$$\Delta T_{\rm m,\,single}=\frac{\left(T_{\rm f,\,s}-T_{\rm w,\,turn}\right)-\left(T_{\rm f,\,out}-T_{\rm w,\,out}\right)}{\ln\left[\left(T_{\rm f,\,s}-T_{\rm w,\,turn}\right)/\left(T_{\rm f,\,out}-T_{\rm w,\,out}\right)\right]} \tag{6}$$

Since the majority of the energy transfer occurs in the two-phase flow region, and for the purpose of convenient expression, we chose the logarithm mean temperature difference in the two-phase flow region $\Delta T_{\rm m,\,two}$ as the logarithm mean temperature difference $\Delta T_{\rm m}$ in the whole heat transfer region.

From the overall heat transfer coefficient, the refrigerant side heat transfer coefficient can be obtained as

$$\frac{1}{H_{\rm f}}=\frac{1}{H_{\rm o}}-\frac{1}{H_{\rm w}}-R_{\rm t} \tag{7}$$

where $R_{\rm t}$ denotes the heat transfer resistance of the wall of the inner tube and $H_{\rm w}$ represents the water side heat transfer coefficient, computed from the Nusselt correlations proposed by Garimella et al. [15] for laminar flow and the Nusselt correlation proposed by Gnielinski [16] for turbulent flow. Those correlations are given as follows:

for $De_{\rm w}<350$,

$$Nu_{\rm w}=0.027De_{\rm w}^{0.94}Pr_{\rm w}^{0.69}\left(\frac{d_{\rm in,\,1}-d_{\rm out,\,2}}{D}\right)^{0.01} \tag{8}$$

for $350<De_{\rm w}<800$,

$$Nu_{\rm w}=0.0018De_{\rm w}^{1.13}Pr_{\rm w}^{0.65}\left(\frac{d_{\rm in,\,1}-d_{\rm out,\,2}}{D}\right)^{0.22} \tag{9}$$

for $De_{\rm w}>800$,

$$Nu_{\rm w}=\frac{(f/8)Re_{\rm w}Pr_{\rm w}}{1.+12.7\sqrt{f/8}\left(Pr_{\rm w}^{2/3}-1\right)} \tag{10}$$

where

$$De_{\rm w}=Re_{\rm w}\left(\frac{d_{\rm in,\,1}-d_{\rm out,\,2}}{D}\right)^{1/2} \tag{11}$$

$$Re_{\rm w}=\frac{\rho_{\rm w}u_{\rm w}\left(d_{\rm in,\,1}-d_{\rm out,\,2}\right)}{\mu_{\rm w}} \tag{12}$$

$$f=0.02985+75.89\left(0.5-a\tan\left(\frac{De_{\rm w}-39.88}{77.56}\right)/\pi\right)\times\left(\frac{d_{\rm in,\,1}-d_{\rm out,\,2}}{D}\right)^{1.45} \tag{13}$$

It is noted that De is Dean number and f is friction factor calculated from the correlation of Xin et al. [17]. Once the Nusselt number is determined, the water side heat transfer coefficient can be computed by means of the following expression:

$$H_{\rm w}=\frac{Nu_{\rm w}\lambda_{\rm w}}{d_{\rm in,\,1}-d_{\rm out,\,2}} \tag{14}$$

Since the water flow is in the annular passage, the hydraulic diameter of the annular cross-section, $d_{\rm in,\,1}-d_{\rm out,\,2}$, is used as the characteristic length in the definitions of dimensionless parameters in Eqs. (8)–(12).

As required for the experimental research, the uncertainty analysis for this experiment has been conducted based on the data deduction equations by using the method recommended by Moffat [18]. The quantities measured directly include refrigerant mass flow rate, water volume flow rate, system pressure and temperature differences. According to the meter specifications, the uncertainty of refrigerant mass flow rate is about 0.1%, and the water volume flow rate uncertainty can be 0.2%. The uncertainty of temperature difference is ± 0.2°C. According to the analysis, the uncertainties of the overall, water side, and refrigerant side heat transfer coefficients are 9.46%, 5.0%, and 15.5%, respectively. The water flow Reynolds number has an uncertainty of 1.53%.

4. Results and discussion

Numerous experimental cases have been run at a fixed system temperature ($T_s = 33°C$) with different water flow rate for different inlet cooling temperatures adjusted to keep the tube wall temperature nearly constant ($T_{wall} = 12°C$ or 22°C) for all test cases. The reason why keeping wall temperature constant is that two-phase flow and condensation heat transfer phenomena in helicoidal pipes are more complicated than in straight pipes because of centrifugal and torsion forces. The condensation heat transfer of R134a in helicoidal pipe varies with its curvature, pitch, pressure drop, void fraction, temperature difference, and flow patterns or flow mass flux. Since we chose the very popular industrial use helicoidal pipe, its curvature and pitch are fixed. During the experimental process we heated and kept R134a at a saturation status ($T_s = 33°C$) to enter the helicoidal pipe. Meanwhile, we adjusted the cooling water flow rate and temperature to make sure the average cooling water temperature was kept constant, so the wall temperature remained nearly the same. Finally, the variables are the cooling water flow rate and corresponding R134a flow rate, and we can get the heat transfer coefficients versus the water or mass flow Reynolds number. This is why we try to keep the temperature of the helicoidal pipe constant.

Since the experimental system was a natural cooling loop (the feature of this loop is to avoid the mixture of refrigerant and oil), the flow rate of the refrigerant and the heat transfer coefficient were both dependent on the cooling condition. In all cases, the refrigerant was cooled below the saturated temperature at the outlet of the test section. Hence, both two-phase and single-phase flow existed on the refrigerant side.

The average heat flux increases with the water flow Reynolds number (see Fig. 3, with $T_s = 33°C$ and $T_{wall} = 12°C$ or 22°C), where the average heat flux was defined as

$$q = \frac{Q}{\pi d_{in,\,2} L} \tag{15}$$

The resulting best-fit lines in the test range, $1500 < Re_w < 9000$, were given

$$\text{For } T_{wall} = 12°C, \quad q = 2.0 Re_w^{0.27} \tag{16}$$

$$\text{For } T_{wall} = 22°C, \quad q = 0.19 Re_w^{0.46} \tag{17}$$

Therefore, at the fixed cooling temperature and saturated refrigerant temperature, the mass flux of the refrigerant flow increased as the water flow Reynolds number increased (see Fig. 4, with $T_s = 33°C$ and $T_{wall} = 12°C$ or 22°C). The mass flux of the refrigerant flow was determined from the following equation:

$$m_f = \frac{F_{f,\,v}\rho_{f,\,v}}{(\pi/4) d_{in,\,2}^2} \tag{18}$$

The corresponding correlations developed from the experimental result in the same range of Re_w were given as

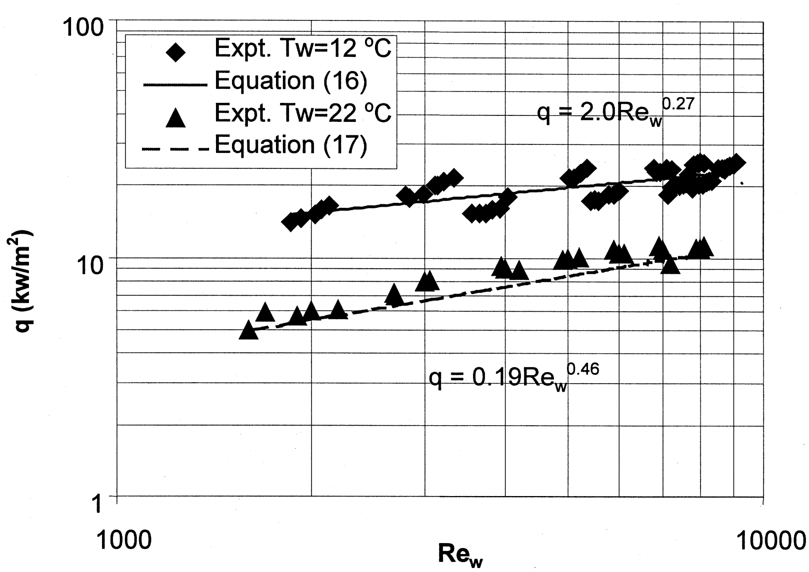

Fig. 3. The relationship between average heat flux on the inner tube wall and the water flow Reynolds number.

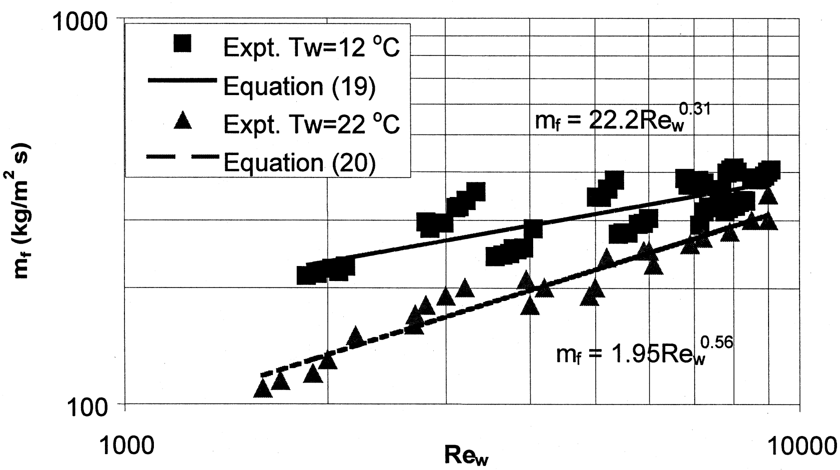

Fig. 4. Variation of the mass flux of refrigerant flow with water flow Reynolds number.

$$\text{For } T_{\text{wall}} = 12°\text{C}, \quad m_{\text{f}} = 22.2Re_{\text{w}}^{0.31} \tag{19}$$

$$\text{For } T_{\text{wall}} = 22°\text{C}, \quad m_{\text{f}} = 1.95Re_{\text{w}}^{0.56} \tag{20}$$

Another observation from Figs. 3 and 4 is that the average heat transfer flux and refrigerant mass flux are significantly higher for the low wall temperature compared to the high wall temperature. At the lowest and highest Reynolds number, they are about 250% and 100% higher, respectively.

The variations of refrigerant side heat transfer coefficients with water flow Reynolds number were presented in Fig. 5 and in the test range $1500 < Re_{\text{w}} < 9000$. They can be expressed by

$$\text{For } T_{\text{wall}} = 12°\text{C}, \quad H_{\text{f}} = 35649Re_{\text{w}}^{-0.38} \tag{21}$$

$$\text{For } T_{\text{wall}} = 22°\text{C}, \quad H_{\text{f}} = 12837Re_{\text{w}}^{-0.32} \tag{22}$$

Fig. 5 shows that with the increase of water flow Reynolds number, the refrigerant heat transfer coefficients decreased. The reason was that on the refrigerant side, as the water flow rate increased, the cooling rate increased, and the refrigerant liquid was cooled even more, resulting in a larger proportion of single-phase flow inside the helicoidal pipe. From knowledge of convective heat transfer, the heat transfer coefficients with phase change are always greater than those of single-phase. Therefore,

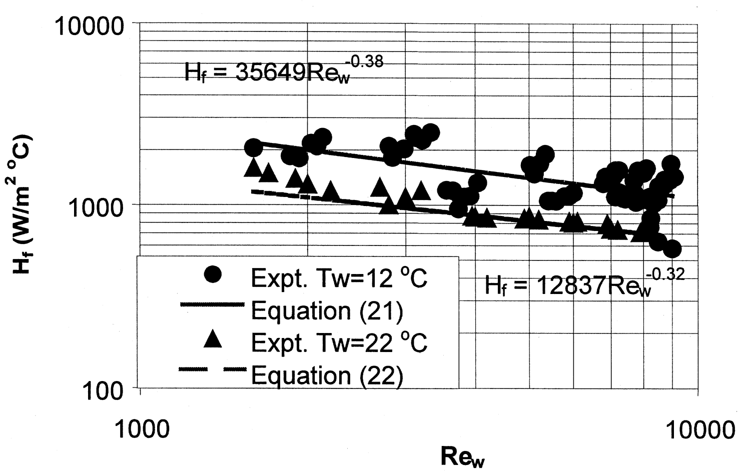

Fig. 5. Refrigerant side heat transfer coefficient vs. water flow Reynolds number.

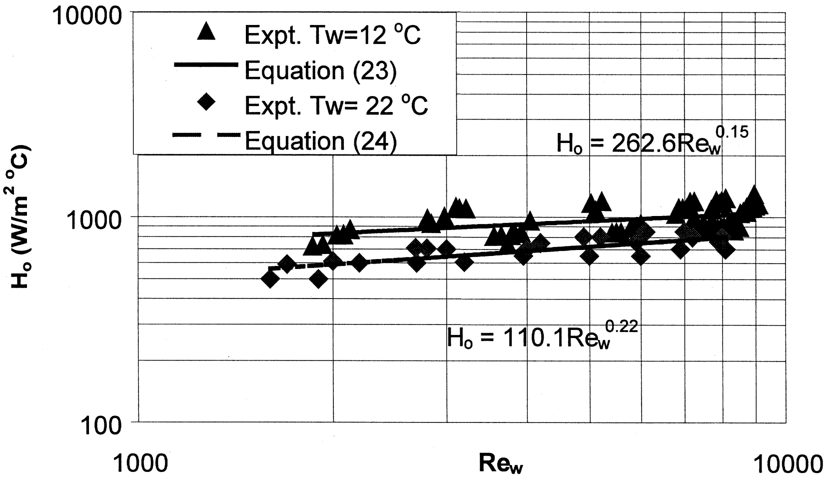

Fig. 6. Overall heat transfer coefficient vs. the water flow Reynolds number.

as the single-phase flow portion inside the tube increased, the heat transfer coefficient on the refrigerant side decreased.

The results of the overall heat transfer coefficient are shown in Fig. 6, which can be predicted

$$\text{For } T_{\text{wall}} = 12°\text{C}, \quad H_o = 262.6 Re_w^{0.15} \tag{23}$$

$$\text{For } T_{\text{wall}} = 22°\text{C}, \quad H_o = 110.1 Re_w^{0.22} \tag{24}$$

where $1500 < Re_w < 9000$.

Fig. 6 shows that as the Reynolds number of water flow increased, the overall heat transfer increased, although the heat transfer coefficient on the refrigerant flow decreased (see Fig. 5). This occurred because the water side heat transfer coefficient increased more than the overall heat transfer coefficient. (In Eqs. (8)–(12), the power index of Re_w is around 1.0, while in Eqs. (23) and (24), it is 0.15 and 0.22.) Thus, the heat transfer coefficient of the refrigerant side decreased (as seen in Figs. 5 and 7). For R134a evaporation inside an axially grooved horizontal tube, Liu [12] mentioned this phenomenon. To the authors' knowledge, this is the first report of the special phenomenon of R134a condensation inside of helicoidal pipe.

In Fig. 7 the resulting best-fit lines in the refrigerant

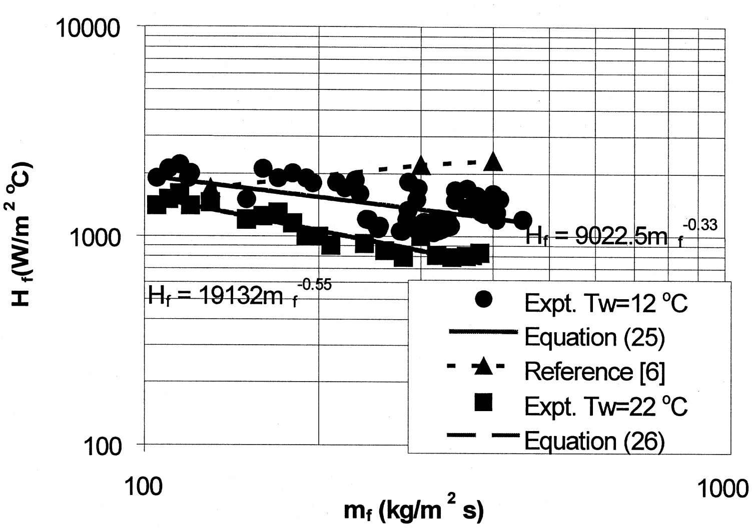

Fig. 7. Refrigerant side heat transfer coefficient vs. the mass flux of the refrigerant flow.

mass flux range of $100 < m_f < 400$ kg/m^2/s to these experimental data were

$$\text{For } T_{\text{wall}} = 12°\text{C}, \quad H_f = 9022.5 m_f^{-0.33} \tag{25}$$

$$\text{For } T_{\text{wall}} = 22°\text{C}, \quad H_f = 19132 m_f^{-0.55} \tag{26}$$

Since the mass flux of the refrigerant flow increased with water flow Reynolds number, as stated above, the increase of the mass flux of the refrigerant flow resulted from the increase in the water flow rate. Therefore, for the same reason explained for Eqs. (21) and (22), with the increase of mass flux of refrigerant, the corresponding heat transfer coefficients decreased.

When compared with data from Eckels and Pate [6] which were represented by a dish line with triangular symbol in Fig. 7, the heat transfer characteristic in helicoidal pipe ($T_s = 33°$C) is as efficient as that of straight tube, where the system condensation temperature was held at 50°C.

The overall heat transfer coefficients versus the mass flux of the refrigerant flow were displayed in Fig. 8, and in the same refrigerant flow mass flux range, they can be expressed by

$$\text{For } T_{\text{wall}} = 12°\text{C}, \quad H_o = 57.6 m_f^{0.49} \tag{27}$$

$$\text{For } T_{\text{wall}} = 22°\text{C}, \quad H_o = 95.4 m_f^{0.34} \tag{28}$$

Similar to data in Fig. 6, with the increase of mass flux, the overall heat transfer coefficients increased. The reason has also been mentioned before.

Due to the variation of refrigerant physical properties, R134a condensation data in Figs. 6–8 demonstrated that the effect of cooling wall temperature on heat transfer coefficients was about 30% (i.e., with the decrease of cooling wall temperature from 22°C to 12°C, the heat transfer coefficients were increased by about 30%), which was not as much as on average heat flux and refrigerant mass flux.

For the present test, the pressure drops versus mass flow of the refrigerant flow mass flux (see Fig. 9) can be expressed as follows:

$$\text{For } T_{\text{wall}} = 12°\text{C}, \quad P_D = 14.2 m_f^{0.093} \tag{29}$$

$$\text{For } T_{\text{wall}} = 22°\text{C}, \quad P_D = 4.5 m_f^{0.26} \tag{30}$$

where $100 < m_f < 400$ kg/m^2/s.

With the increase of refrigerant flow mass flux, the pressure drops increased but very slowly (the power index is just about 0.11 in Eqs. (29) and (30)). By the way, the effect of cooling wall temperature on system pressure drops was about 30%, which was almost the same as the effect on heat transfer coefficients.

Compared with results from Eckels and Pate [6] shown by dish line with triangular symbol in Fig. 9 (the data of microfin with $t_s = 40°$C were chosen and transferred from total pressure drop to per unit pressure drop), the pressure drop in helicoidal pipe was greater than that of microfin straight tube. However, with the increase of flow mass flux, the difference was getting smaller and smaller.

The experimental data were rearranged to form dimensionless groups as shown in Fig. 10. The vapor quality at the entrance and exit of the helicoidal pipe

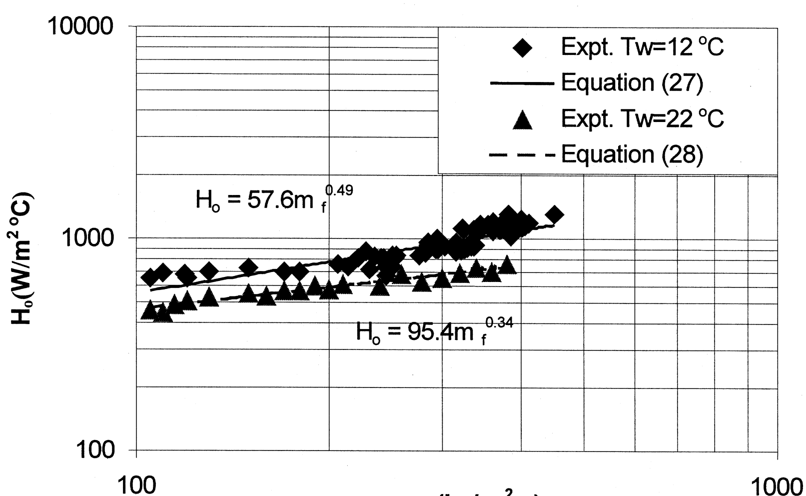

Fig. 8. Overall heat transfer coefficient vs. the mass flux of the refrigerant flow.

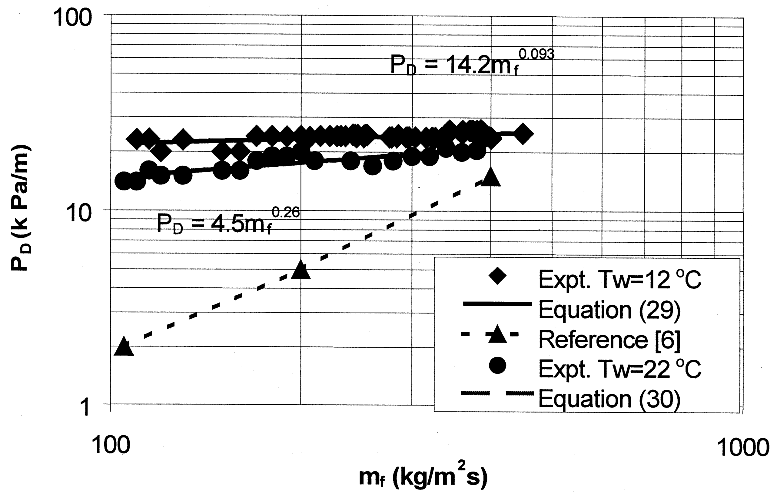

Fig. 9. R134a pressure drop as a function of mass flux of the refrigerant flow.

was defined in terms of the enthalpies of saturated vapor and liquid,

$$x = \frac{h - h_l}{h_{f,\,v} - h_l} \tag{31}$$

In all the present tests, due to the relatively long length of the cooling tube, the variation of vapor quality was from 1 to 0. This phenomenon was consistent with the flow patterns observed from the glass watch window.

When the average vapor quality was used in the data reduction process, the heat transfer coefficient in the range of $1100 < Re^* < 2500$ could be correlated in the form:

$$\frac{Nu}{Pr^{0.4}} = 2.3(Re^*)^{0.94} \tag{32}$$

where

$$Nu = \frac{H_f d_{in,\,2}}{\lambda} \tag{33}$$

$$Re^* = \frac{m x d_{in,\,2}}{\mu_l \sqrt{\rho_l/\rho_v}} \tag{34}$$

For the purpose of fair comparison, non-dimension numbers were used. The dash line with triangular symbol in Fig. 10 represented the condensing result of R134a inside a grooved horizontal tube [12].

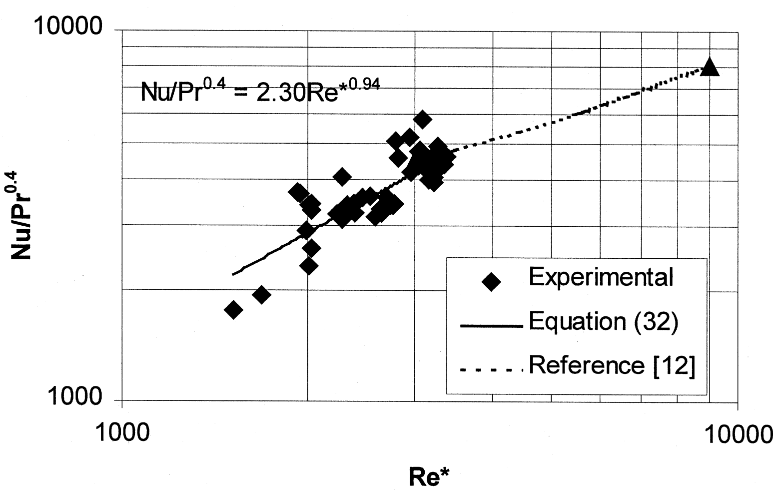

Fig. 10. R134a condensing heat transfer characteristic in helicoidal pipe.

Obviously, helicoidal pipe performs almost the same heat transfer characteristic as horizontal tube when it is grooved. This was due to the existence of secondary flow in helicoidal pipe, and it can be concluded that secondary flow played an important role in the process of R134a condensation.

A modified Reynolds number Re^* was chosen to reduce the data. The purpose of this plot is to compare the present results with the previous author at different condensation temperatures. Actually, the modified Reynolds number is different from the regular Reynolds number Re_w. It represents the influence of average vapor quality and mass flux. When it increases with the mass flux invariable, the average vapor quality also increases. For the present study, it means the two-phase proportion increases; therefore, the heat transfer coefficients increase. It agrees with the previous discussion. When the modified Reynolds number increases with the average vapor quality invariable, the mass flux increases. Here, we have two methods to increase the mass flux: one is to increase the flow speed of cooling water, and the other is to decrease the temperature of cooling water. From the experiment results, cooling water temperature affects the heat transfer coefficients much more than cooling water flow speed, which is inversely proportional to refrigerant side heat transfer coefficients. It also supports the previous discussion.

The coefficients and power indices in the above equations were determined by using the least-squares method, and the maximum deviation from the best-fit lines to these equations was within −37.3% to 35.7%.

5. Concluding remarks

Condensation heat transfer of the alternative refrigerant, R134a, inside a long helicoidal pipe at a fixed system temperature ($T_s = 33°C$) and tube wall temperature ($T_{wall} = 12°C$ and 22°C) has been experimentally investigated. The results were presented to illustrate the heat transfer characteristics of R134a. In particular, the heat transfer coefficient variations for R134a versus the coolant flow rate have been analyzed. It was found that the average heat flux of the refrigerant flow increases with the water flow rate. A special heat transfer phenomenon was reported; i.e., the heat transfer coefficients on the refrigerant side decreased as the mass flux of the refrigerant flow (or cooling water flow Reynolds number) increased, although the overall heat transfer coefficient increased. The vapor–liquid two-phase and single liquid phase coexisted in the helicoidal pipe in the tested cases. The refrigerant was cooled below the saturated temperature at the exit of the helicoidal pipe. In the meanwhile, the R134a flow pressure drop and the condensing heat transfer characteristic in helicoidal pipe were presented. Experimental results showed that cooling wall temperature had nearly the same effect on heat transfer as on system pressure drop (about 30% for cooling wall temperature from 12°C to 22°C). Finally, the helicoidal pipe heat transfer characteristic can be expressed as

$$\frac{Nu}{Pr^{0.4}} = 2.3(Re^*)^{0.94} \tag{35}$$

where $1100 < Re^* < 2500$.

References

[1] Y.G. Bokhanovskiy, Heat transfer for Freon-12, Freon-22, and their mixtures in a coiled tube condenser, Heat Transfer Soviet Research 12 (1980) 43–45.
[2] W.F. Stocker, E. Koronta, Condensing coefficients when using refrigerant mixture, Transactions ASHRAE 91 (1985) 1351–1367.
[3] T.N. Tandon, H.K. Varuma, C.P. Gupta, Prediction of flow patterns during condensation of binary mixtures in a horizontal tube, ASME Journal of Heat Transfer 107 (1985) 424–430.
[4] T.N. Tandon, H.K. Varuma, C.P. Gupta, Generalized correlation for condensation of binary mixtures inside a horizontal tube, International Journal of Refrigeration 9 (1986) 134–136.
[5] S. Mochizuki, T. Inove, M. Tominaga, Condensation of nonazeotropic binary mixtures in a horizontal tube, Transactions JSME Part B 54 (1988) 1796–1801.
[6] S.J. Eckels, M. Pate, Evaporation and condensation of R134a and CFC-12 in a smooth tube and a micro-fin tube, Transactions ASHRAE 97 (1991) 71–81.
[7] K. Torikoshi, K. Kawabata, T. Ebisu, Heat transfer and pressure drop characteristics of R134a in a horizontal heat transfer tube, in: Proceedings of 1992 International Refrigeration Conference, vol. 1, 1992, pp. 167–176.
[8] K. Torikoshi, T. Ebisu, Evaporation and condensation heat transfer characteristics of R134a, R32, and a mixture of R32/R134a inside a tube — part I, Transactions ASHRAE 99 (1993) 90–96.
[9] T. Ebisu, K. Torikoshi, In-tube condensation of alternative refrigerants, in: Proceedings of Condensation and Condenser Design Conference, St. Augustine, FL, 1993, pp. 593–600.
[10] M. Uddin, J. Patrick, A. Newlin, Variation of local condensation heat transfer coefficient for R134a in helically coiled tubes, ASME Journal 94-WA/HT-4 (1994).
[11] X. Liu, Modified LMTD method for two-phase heat transfer and application in heat exchangers, in: Proceedings of 1996 International Refrigeration Conference, Purdue University, West Lafayette, IN, 1996, pp. 145–150.
[12] X. Liu, Condensing and evaporating heat transfer and pressure drop characteristics of HFC-134a and HCFC-22, Journal of Heat Transfer 119 (1997) 158–163.

[13] A.A.S. Huerta, S.L. Braga, J.A.R. Parise, Simulation of the effects of oil on heat transfer during condensation of refrigerants R-12 and R-134a, in: Proceedings of 11th International Heat Transfer Conference, vol. 61, 1998, pp. 421–426.

[14] ASHRAE, Handbook of Fundamentals, American Society of Heating, Refrigerating, and Air Conditioning Engineering, Atlanta, GA, 1997.

[15] S. Garimella, D.E. Richards, R.N. Christensen, Experimental investigation of heat transfer in coiled annular ducts, ASME Journal of Heat Transfer 110 (1988) 329–336.

[16] V. Gnielinski, Heat transfer and pressure drop in helically coiled tubes, in: Proceedings of the International Meeting on Reactor Heat Transfer, Karlsruhe, Germany, 1986. Paper No. 16, 1986, pp. 351–372.

[17] R.C. Xin, A. Awwad, Z.F. Dong, M.A. Ebadian, An experimental study of single-phase and two-phase flow in annular helicoidal pipes, National Heat Transfer Conference 8 (1996) 11–17.

[18] R.J. Moffat, Describing uncertainties in experimental results, Experimental Thermal Fluid Science 1 (1988) 3–7.